International Journal of Pharmaceutics 414 (2011) 148–156

Contents lists available at ScienceDirect

International Journal of Pharmaceutics

journal homepage: www.elsevier.com/locate/ijpharm

Comparison of mesoporous silicon and non-ordered mesoporous silica materials as drug carriers for itraconazole

Päivi Kinnari[a], Ermei Mäkilä[b], Teemu Heikkilä[b], Jarno Salonen[b], Jouni Hirvonen[a], Hélder A. Santos[a,*]

[a] Division of Pharmaceutical Technology, Faculty of Pharmacy, University of Helsinki, FI-00014, Finland
[b] Laboratory of Industrial Physics, Department of Physics and Astronomy, University of Turku, FI-20014, Finland

ARTICLE INFO

Article history:
Received 21 March 2011
Received in revised form 4 May 2011
Accepted 5 May 2011
Available online 12 May 2011

Keywords:
Drug loading
Drug release
Itraconazole
Silica gel
Mesoporous silicon
Dissolution

ABSTRACT

Mesoporous materials have an ability to enhance dissolution properties of poorly soluble drugs. In this study, different mesoporous silicon (thermally oxidized and thermally carbonized) and non-ordered mesoporous silica (Syloid AL-1 and 244) microparticles were compared as drug carriers for a hydrophobic drug, itraconazole (ITZ). Different surface chemistries pore volumes, surface areas, and particle sizes were selected to evaluate the structural effect of the particles on the drug loading degree and on the dissolution behavior of the drug at pH 1.2. The results showed that the loaded ITZ was apparently in amorphous form, and that the loading process did not change the chemical structure/morphology of the particles' surface. Incorporation of ITZ in both microparticles enhanced the solubility and dissolution rate of the drug, compared to the pure crystalline drug. Importantly, the physicochemical properties of the particles and the loading procedure were shown to have an effect on the drug loading efficiency and drug release kinetics. After storage under stressed conditions (3 months at 40 °C and 70% RH), the loaded silica gel particles showed practically similar dissolution profiles as before the storage. This was not the case with the loaded mesoporous silicon particles due to the almost complete chemical degradation of ITZ after storage.

1. Introduction

In the last decade the applications of mesoporous based-materials as potential drug delivery systems have grown exponentially, in particular in the field of oral drug delivery (Wang, 2009). Most of the new drug molecule candidates suffer from poor oral bioavailability, and thus, there is a great need for drug delivery systems capable of improving the physicochemical properties (e.g., dissolution and solubility) of drugs.

Recently, the application of mesoporous silica and silicon particles has been widely studied as prospective oral drug delivery vehicles to improve dissolution properties of hydrophobic drug molecules. Many of those studies have been performed with MCM-41, SBA-15 and TUD-1 silica-based mesoporous materials (Ambrogi et al., 2007, 2008; Charnay et al., 2004; Heikkilä et al., 2007a,b; Horcajada et al., 2004, 2006; Mellaerts et al., 2007, 2008a,b; Muñoz et al., 2003; Van Speybroeck et al., 2009, 2010). In addition to mesoporous silica materials, mesoporous silicon particles with different surface modifications have also been extensively studied as drug carriers with promising results (Bimbo et al., 2011; Foraker et al., 2003; Heikkilä et al., 2007b; Kaukonen et al., 2007; Limnell et al., 2007; Salonen et al., 2005; Wang et al., 2010). The ability of mesoporous materials to enhance the solubility and dissolution rate of the incorporated drug is based, e.g. on their small pores (often of 2–10 nm in diameter), which are only a few times larger than the dimensions of drug molecules, thus preventing drug crystallization (Salonen et al., 2008).

In practice, the porous silica and silicon materials differ in their fabrication techniques; porous silica materials are synthesized through a so-called "bottom-up" approach, whereas porous silicon (PSi) materials are produced by a so-called "top-down" approach (Salonen et al., 2008). In the field of drug research, MCM-41 and SBA-15 are the most studied ordered mesoporous silica materials, which contain very unidirectional and uniform pore channel structures (Beck et al., 1992; Zhao et al., 1998). On the other hand, silica gels or xerogels differ from the ordered mesoporous silica due to their disordered pore structure, and these materials have also been studied as systems for sustained and controlled drug release (Ahola et al., 2000; Böttcher et al., 1998; Chen et al., 2004; Kortesuo et al., 2000, 2001; Radin et al., 2001; Santos et al., 1999), as well as for enhanced drug dissolution (Limnell et al., 2011; Monkhouse and Lach, 1972; Narurkar and Jarowski, 1983; Yang et al., 1979). In addition, porous silica materials are commonly used as food additives and pharmaceutical excipients (W.R. Grace and Co.-Conn., 2006).

The surface chemistries of the ordered and disordered silica materials are similar, consisting of siloxane groups (–Si–O–Si–),

* Corresponding author. Tel.: +358 9 191 59160; fax: +358 9 191 59144.
E-mail address: helder.santos@helsinki.fi (H.A. Santos).

0378-5173/$ – see front matter © 2011 Elsevier B.V. All rights reserved.
doi:10.1016/j.ijpharm.2011.05.021

with the oxygen on the surface, and of three forms of silanol groups (–Si–OH) (Rigby et al., 2008; Zhao et al., 1997; Zhuravlev, 2000). Like silica gels, PSi particles also have irregular pore structure, but the surface of the as-anodized, hydrogen-terminated PSi is not stable, and thus, there is a need for subsequent surface modification (Salonen and Lehto, 2008). The most common surface treatments of PSi are oxidation (thermally oxidized-PSi, TOPSi) and stabilization by thermal carbonization (TCPSi), or hydrocarbonization (THCPSi) (Bimbo et al., 2010; Kaukonen et al., 2007; Kilpeläinen et al., 2009; Limnell et al., 2007; Salonen et al., 2005; Santos et al., 2010; Wang et al., 2010), which render the PSi materials hydrophilic or hydrophobic surface properties.

Despite the active research in the drug delivery field by means of porous materials, there is still a lack of comparison between the mesoporous silicon and non-ordered mesoporous silica materials. It has been shown that several properties of the mesoporous materials affect the loading degree and release rate of the incorporated drug, such as the surface area, pore size, total pore volume, pore geometry and surface chemistry (Andersson et al., 2004; Charnay et al., 2004; Heikkilä et al., 2007b; Salonen et al., 2005; Song et al., 2005). The most common drug loading method for porous materials is by immersion, which is based on the adsorption of drug molecules from a concentrated drug solution into the pore walls. However, thorough and systematic studies to evaluate the ideal drug loading procedures and the most suitable properties of the mesoporous materials for the drug loading and release are still required.

In this study, we have investigated the effect of the surface chemistry of mesoporous silica and silicon materials on the itraconazole (ITZ, a hydrophobic poorly soluble drug molecule) loading, and consequently, on the release and dissolution behavior of ITZ. Two different mesoporous silicon, TOPSi and TCPSi, and non-ordered mesoporous silica, Syloid AL-1 and 244, materials were used and compared. The stability and drug release profiles of the ITZ-loaded materials were also assessed after 3 months storage (40 °C and 70% RH).

2. Materials and methods

2.1. Materials

Syloid 244 FP EU and Syloid AL-1 FP were kindly provided by Grace Davison (Grace GmbH & Co. KG, Germany) and used as received.

The PSi materials were fabricated as described in detail elsewhere (Salonen et al., 2002; Riikonen et al., 2009; Santos et al., 2010). Briefly, the PSi particles were prepared by anodizing silicon wafers [boron doped, p^+-type Si(1 0 0) wafers with a resistivity of 0.01–0.02 Ω cm] with a current density of 50 mA/cm^2 in hydrofluoric acid (Merck, 38%)–ethanol (Altia Oyj, 99.5%) mixture (1:1). The free-standing films were obtained by sharply increasing the current density in the end of the etching process. After the anodization, the free-standing PSi films were ball milled and dry-sieved with a mesh with nominal pore sizes of 25 and 75 μm. The milling and sieving cycles were repeated several times to achieve the desired particle sizes. After the dry-sieving, the particles were rinsed with ethanol on the mesh to remove small agglomerates. Before thermal carbonization the sieved particles were treated with HF to remove the oxides formed during the milling. All the particles were dried for at least 1 h at 65 °C. PSi microparticles of two different surface chemistries were produced: thermally carbonized PSi (TCPSi) and thermally oxidized PSi (TOPSi).

ITZ was used as received (Apotecnia, Spain) and stored in ambient conditions protected from light. ITZ is a weak base (pK_a = 2 and 3.7), an antifungal compound belonging to the Biopharmaceutical Classification System Class II, and its high crystal lattice energy and hydrophobic nature make it extremely water insoluble and pH-dependent (~5 μg ml^{-1} at pH 1 and ~1 ng ml^{-1} at pH 7) (Van Speybroeck et al., 2010; Peeters et al., 2002).

2.2. Loading of ITZ into the porous materials

Loading of the particles was performed by the immersion method, in which the particles (100 mg) were immersed into a concentrated ITZ solution in 5 ml of dichloromethane (DCM; Sigma–Aldrich Chemie GmbH, Germany). The drug loading procedures were performed with two different drug concentrations for the silica particles: 235.5 (denoted as "high") and 117.8 mg/ml (denoted as "low"). Silicon particles were loaded with the low concentration. The high concentration was selected according to the pre-determined highest soluble amount of ITZ in the solvent and the low concentration was selected as half of the highest soluble amount. The particle suspensions were mixed and stirred for 24 h (high ITZ concentration) or for 3 h (low ITZ concentration) at room temperature protected from the light. To evaluate the effect of the particle–solvent interactions, reference particles were also immersed into the loading solvent without ITZ. After the loading, the samples were vacuum filtrated from the solution with a polypropylene membrane filter of 0.45 μm nominal pore size (Pall Life Sciences, USA). To ensure complete elimination of the solvent, the loaded particle samples were dried at 50 °C for 2 h.

To investigate the stability of the loaded particles and possible degradation of the loaded ITZ, both silica and silicon ITZ-loaded particles were also stored under stressed conditions for 3 months (40 °C and 70% RH).

2.3. Physicochemical characterization of the mesoporous microparticles

The physicochemical properties (specific surface area, pore volume and pore diameter) of the unloaded particles were characterized by N_2 sorption method with a Tristar 3000 (Micromeritics, GA, USA) instrument at −196 °C. The specific surface areas of the particles were determined from the adsorption branch of the nitrogen isotherm using Brunauer–Emmett–Teller (BET) theory. The pore volume and the average pore diameter were calculated from the desorption branch of the isotherm with Barrett–Joyner–Halenda (BJH) theory.

Fourier transform infrared spectrometer (FTIR) was used to examine the effect of drug loading on the chemical structure of the particles, and also to evaluate the success of the drying treatment. The FTIR studies were carried out using a Bruker VERTEX 70 series FTIR spectrometer (Bruker Optics, Germany) with a horizontal ATR sampling accessory (MIRacle, Pike Technology, Inc.). In all measurements the resolution used was 4 cm^{-1}. Opus 5.5 software was used for collecting the measured data.

Differential scanning calorimeter (DSC) and X-ray powder diffractometer (XRPD) were used to study the state of the loaded drug (crystalline or amorphous). The DSC analysis was carried out with Mettler Toledo DSC823e (Mettler Toledo, Columbus, OH) using a heating rate of 10.0 °C/min under N_2 gas purge of 50 ml/min, in 40 μl aluminum sample pans with holes. The heating range for the measurements was selected from 25 to 220 °C. STARe software was used for collecting the measured data. The XRPD measurements were performed using a variable temperature XRPD (VT-XRPD, Bruker AXS D8, Karlsruhe, Germany). The experiments were performed in symmetrical reflection using Cu Kα-radiation. The scattered intensities were measured with a scintillation counter. The angular range used was from 5° to 35° with steps of 0.02° and measuring times of 0.5 s/step. Samples were heated to 25, 49, 105, 110, 135, 143, 170 and 220 °C with a heating

Table 1
Physical characterization of the mesoporous silica and silicon microparticles.

Particles	Particle size (μm)	Surface area (m^2/g)[b]	Pore volume (cm^3/g)[c]	Average pore diameter (nm)[d]
Syloid AL-1	6.5–8.1[a]	683 ± 11	0.130 ± 0.005	3.2 ± 0.02
Syloid 244	2.5–3.7[a]	311 ± 14	1.42 ± 0.04	19.0 ± 1.1
TCPSi	25–75	253 ± 5	1.06 ± 0.04	12.9 ± 0.5
TOPSi	25–75	226 ± 6	0.73 ± 0.04	9.1 ± 0.5

[a] Product specifications, Grace Davison Discovery Sciences, Grace GmbH & Co. KG.
[b] BET surface area.
[c] BJH total pore volume.
[d] BJH average pore diameter.

rate of 0.167 °C/s. VT-XRPD measurements were performed for the ITZ-loaded particles and also for pure ITZ.

The surface morphologies of the unloaded and loaded particles were studied by scanning electron microscope (SEM; Zeiss DSM 962, Carl Zeiss, Oberkochen, Germany). The samples were sputter coated with platinum before the imaging.

2.4. Determination of the ITZ loading degree

The total amount of ITZ loaded in the silica and silicon particles, and the ITZ amount after storage in the particles were quantified by HPLC. Particle samples of 1–2 mg were extracted in 10 ml of methanol under vigorous stirring for at least 45 min.

Drug concentrations in the samples were analyzed with Agilent 1100 series HPLC system (Agilent Technologies, Germany) consisting of a binary pump (Agilent G1312A), a column compartment (Agilent G1316A), a multi-wavelength detector (Agilent G1365B), a well plate autosampler (Agilent G1367A) and a degasser (Agilent G1379A). The separation of ITZ was achieved by using a Gemini C18 column (Gemini-NX, 3 μm C18, 110 Å; Phenomenex, USA) and a flow rate of 1 ml/min. The mobile phase during determination (λ = 261 nm, retention time ~1.9 min) consisted of acetonitrile and 0.1% trifluoroacetic acid pH 2.0 (55:45). Injection volumes of 20 μl were used for analysis. The determined loading degrees were further used for calculation of percentage-released drug amount in the dissolution tests.

2.5. Drug dissolution and release experiments

The release of ITZ from the porous silica and silicon particles was compared with the dissolution of pure crystalline ITZ. The dissolution tests were carried out with the Ph. Eur. paddle apparatus method (Sotax AT7, Sotax AG, Basel, Switzerland) at 250 rpm with 500 ml of pH 1.2 medium (hydrochloride acid buffer, Ph. Eur. 6.8) at 37 °C. The loaded particles (<0.7 mg) were weighted in open gelatin capsules and a small magnet was used as a sinker inside each capsule. For each time point, 1 ml of dissolution medium was collected during the experiments and replaced with 1 ml of fresh pre-warmed (37 °C) medium.

The tests were performed under sink conditions, meaning that the volume of the medium was at least three times greater than that required to form a saturated solution of the drug. All the experiments were performed for 120 min and were repeated for at least four times. All the aliquots collected were analyzed with HPLC in order to quantify the amount of ITZ released over time.

3. Results and discussion

3.1. Characterization of the mesoporous materials

The commercially available mesoporous silica microparticles used in this study differed from each other in their particle size, surface area, pore size and pore volume. Fig. S1 shows the SEM pictures of the mesoporous particles. It can be observed that the PSi particles are larger and have more angular structures than the mesoporous silica particles that are more spherical-like. The Syloid 244 and Syloid AL-1 are amorphous gel-type silicas with typically randomly oriented pores. Syloid AL-1 particles have a surface area and particle size more than twice larger than Syloid 244 particles, whereas Syloid 244 particles have a much larger pore volume and average pore diameter than Syloid AL-1 particles (Table 1). The surface areas of the mesoporous silicon particles are similar and as large as the surface area of Syloid 244 particles. The pore volumes and the average pore diameters of TCPSi particles are slightly larger compared with those of TOPSi. The pore volumes and pore diameters of Syloid 244 particles are the largest of all the studied particles, which may allow higher payloads of drug molecules. The size of one ITZ molecule is about 0.69 nm × 0.93 nm × 2.97 nm (Mellaerts et al., 2008b) and, thus, there may be enough space in the wide pores of Syloid 244 and PSi particles for ITZ to crystallize, which can decrease the drug release rate (Riikonen et al., 2009).

The two PSi materials have different surface chemical structures; TCPSi particles have carbon atoms attached on the silicon surface, while TOPSi particles have siloxane and a few silanol groups on their surface (Salonen et al., 1997a, 2002). As a result of their surface chemical structure, these mesoporous silicon particles are hydrophilic in nature and rather stable. Amorphous silica materials have a large number of silanol groups on their surface which also render them hydrophilic properties (Zhuravlev, 1987).

No structural changes were observed in the FTIR spectra on the surface of the mesoporous silica or silicon particles after treatment with DCM, which also indicates that the drying process of the particles was sufficient to remove any excess of the organic loading solvent (data not shown). The FTIR spectrum of Syloid AL-1 (Fig. 1) showed a broad band in the range 3550–2500 cm^{-1} typical for the free hydroxyl groups, free silanols, and vicinal silanols (Jesionowski et al., 2004). Because the siloxane groups provide a much stronger intensity band (broad band from 1300 to 1000 cm^{-1})

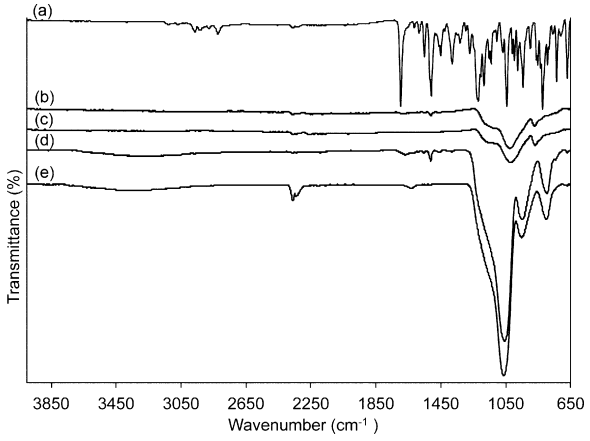

Fig. 1. FTIR spectra of pure ITZ (a), ITZlow + TOPSi (b), unloaded TOPSi (c), ITZlow + SylAL-1 (d), and unloaded ITZlow + SylAL-1 (e).

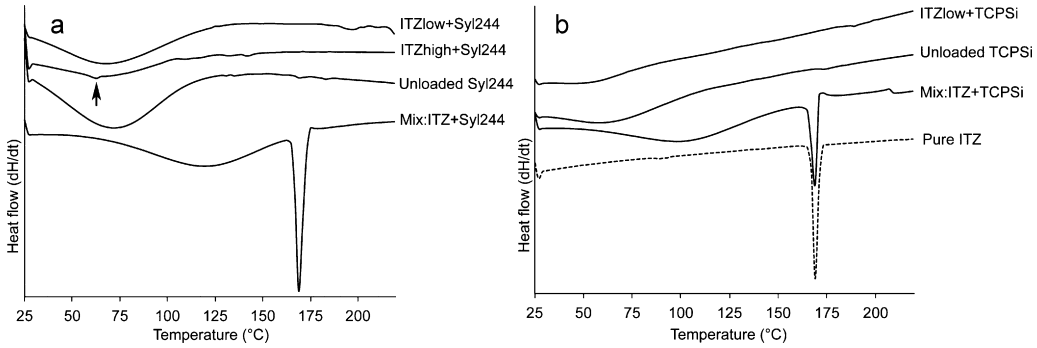

Fig. 2. DSC thermograms of loaded and unloaded Syloid 244 (a) and TCPSi (b) particles, pure ITZ (b), and physical mixtures of ITZ and Syloid 244 (a) or TCPSi particles (b). The solid black arrow indicates the position of the Tg of ITZ. Endothermic signals are pointed downwards.

than the silanol groups, the later groups cannot easily be seen at this scale. The FTIR spectrum of TOPSi exhibited a broad band around 1000 cm^{-1} typical for Si–O–Si (siloxane) stretching bonds (Salonen et al., 1997b).

In addition, no extra bands in the FTIR spectra of the loaded Syloid AL-1 and TOPSi particles were observed after ITZ loading, which indicates that the surface of the particles remained unchangeable after loading. Some of the bands characteristic to ITZ can be distinguished at 1700 and 1510 cm^{-1}, which also appear in the FTIR spectra of the loaded microparticles (the absorption bands of ITZ are however weaker due to the low weight ratio of the drug in the particles). Similar results were also obtained for Syloid 244 and TCPSi particles (data not shown).

All the loaded samples were also analyzed with DSC and compared to unloaded mesoporous particles, pure ITZ and physical mixtures of ITZ and mesoporous particles. The physical mixtures of ITZ and the mesoporous particles were prepared by mixing the crystalline ITZ and the particles with weight ratios that correspond to the lowest ITZ loading degrees obtained in the particles: ITZlow + SylAL-1 (20% of ITZ: 80% of particles), ITZlow + Syl244 (20:80%), ITZlow + TOPSi (10:90%) and ITZlow + TCPSi (10:90%). Fig. 2 shows the DSC thermograms of both pure ITZ and the physical mixtures with the corresponding melting transition of crystalline ITZ at 168 °C. No ITZ melting point was detected for the loaded mesoporous particles, which indicates that the drug loaded was in an amorphous form after the loading. A rather small glass transition (Tg) around 60 °C (Fig. 2, black arrow) was, however, observed for the sample ITZhigh + Syl244. Mellaerts and co-workers (2007, 2008a,b) have demonstrated that ITZ is molecularly dispersed as bulk phase transitions, including endothermic transitions of amorphous ITZ (at 60, 70 or 90 °C), and melting of crystalline ITZ are not shown in the DSC thermograms. The XRPD patterns (Fig. 3) of the ITZ-loaded mesoporous silica particles and pure ITZ at 25 °C supported the DSC results and did not show any diffraction peaks

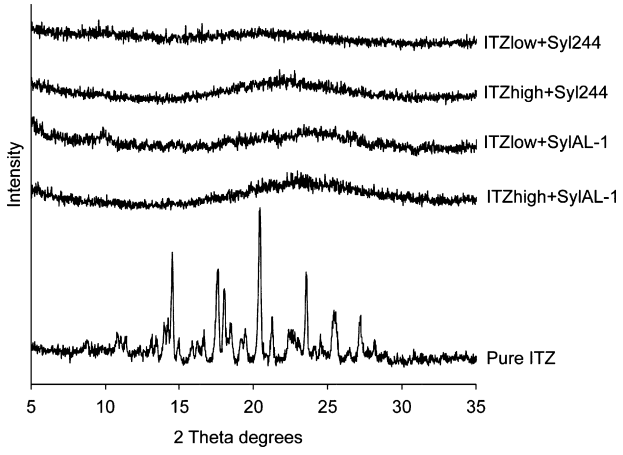

Fig. 3. XRPD patterns at 25 °C of the ITZ-loaded silica particles and pure ITZ.

characteristic for the crystalline form of ITZ. The diffraction pattern of pure ITZ showed the typical reflections of crystalline ITZ from 25 °C to 143 °C and from 170 °C to 220 °C ITZ was melted (data not shown). Heating of the loaded mesoporous materials did not elicit any change in their diffraction patterns (data not shown).

In addition, SEM pictures did not show any significant changes in the morphology and shape of the particles before and after loading (data not shown).

3.2. Quantification of ITZ loaded into the mesoporous particles

In addition to the determination of the loading degrees by HPLC, the theoretical maximum loading degrees and monolayer capacities were also calculated for all the particles (Table 2). The theoretical maximum loading degrees were calculated based on

Table 2
Abbreviations, total ITZ content of the loaded particles determined by HPLC (w-%, $n \geq 4$) before and after storing the particles at 40 °C and 70% RH for 3 months (average ± SD), theoretical maximum loading degrees and monolayer capacities.

Abbreviation of the loaded particles	Particles	c_{drug} (mg/ml)[a]	Loading time (h)	Load (w-%)[b]	$Amount_{stressed}$ (w-%)[c]	Theor max load (w-%)[d]	Theor monolayer cap (w-%)[e]
ITZhigh + Syl244	Syloid 244	235.5	24	32.8 ± 1.4	30.4 ± 8.7	66.1	14.0
ITZlow + Syl244	Syloid 244	117.8	3	21.9 ± 1.5	16.6 ± 1.2		
ITZhigh + SylAL-1	Syloid AL-1	235.5	24	25.1 ± 8.6	21.3 ± 0.3	15.1	30.7
ITZlow + SylAL-1	Syloid AL-1	117.8	3	21.0 ± 3.4	19.1 ± 0.4		
ITZlow + TCPSi	TCPSi	117.8	3	11.3 ± 1.3	1.3 ± 0.05	59.2	11.4
ITZlow + TOPSi	TOPSi	117.8	3	11.2 ± 1.7	0.10 ± 0.09	50.0	10.1

[a] Drug concentration of the loading solution.
[b] Loading degrees before storage.
[c] Amount of drug remained after storage under stressed conditions (40 °C/70% RH).
[d] Theoretical maximum loading degree (Rowe et al., 2003).
[e] Theoretical monolayer capacity (Mellaerts et al., 2007).

the pore volume and on the density of crystalline ITZ (Rowe et al., 2003). The crystalline bulk drug has been shown to have a slightly higher density than the amorphous bulk drug, however the differences are not significant (Hancock et al., 2002). The monolayer capacity of ITZ on the particles' surface was calculated based on the drug molecule size and the BET surface area of the particles which covers both the mesopore surface and the outer surface (Mellaerts et al., 2007). The monolayer capacity is useful for the comparison of the results and it has been associated with the generation of maximum ITZ-dissolution rate enhancement.

The amount of ITZ loaded into the mesoporous silica microparticles with low-loading concentrations of ITZ, ITZlow + SylAL-1 (21.0 w-%) and ITZlow + Syl244 (21.9 w-%), was higher than that into the mesoporous silicon microparticles (about 11% for both TOPSi and TCPSi) using the same loading procedure. Interestingly, the two Syloids showed similar loading degrees when the low-loading concentrations of ITZ were used, despite their significant differences in pore size, surface area and pore volume. As expected, at high-loading concentrations of ITZ for 24 h, the loading degrees of Syloid AL-1 and 244 were increased to 25.1 and 32.8 w-%, respectively.

Apparently, the affinity of ITZ towards the Syloid particles was higher than towards the PSi microparticles, despite the larger pore sizes of PSi compared to Syloid AL-1. The difference in the loading efficiency between the mesoporous silica and silicon may partly result from the fact that the mesoporous surfaces of silica particles contain large amounts of silanol groups that are favorable for interaction with ITZ through hydrogen bonds (Horcajada et al., 2006; Song et al., 2005; Zhuravlev, 1987). This may be important to achieve higher drug payloads. It has been shown that attractive interactions between the solvent and the drug molecule or between the solvent and the adsorbent can weaken the drug adsorption to the particle surfaces due to possible competition on the adsorption sites (Fisher et al., 2003; Rosenholm and Lindén, 2008). Thus, weaker PSi–ITZ interactions and stronger solvent–ITZ or solvent–PSi interactions could also affect the ITZ-loading into PSi.

The different pore geometry could also explain some of the differences observed in the loading degrees between the mesoporous silica and silicon particles. PSi particles, produced with high-doped Si substrate, have branched, fir tree-type pore structures (Salonen and Lehto, 2008), whereas silica gels are composed of a vast network of interconnected pores (Nakanishi et al., 2000). Therefore, the mesopore network of the mesoporous silica materials is possibly more accessible (Heikkilä et al., 2007a; Song et al., 2005) for efficient ITZ adsorption than the pore structure of PSi. In addition, the smaller particle sizes of Syloids could allow more efficient loading of the drug than the large PSi particles (Aerts et al., 2007).

The variation observed in the loading degrees of Syloid AL-1 particles (Table 2) could be attributed to the fact that part of the ITZ molecules did not physically fit inside the pores (only slightly larger than the ITZ molecule) and the drug was possibly adsorbed partially on the surface of the particles (Wang and Li, 2006). However, since the DSC and XRPD results did not show any melting of crystalline ITZ (Figs. 2 and 3) it is possible that if adsorbed on the outer surface of the particles, ITZ was likely molecularly dispersed and did not form a clear crystal structure. This is further corroborated by the low theoretical ITZ-loading degree (15.1 w-%) and the large theoretical monolayer capacity (30.7 w-%) of Syloid AL-1 particles, which also indicates that ITZ could be molecularly dispersed on the surface of the Syloid AL-1 particles as a monolayer (Mellaerts et al., 2007). Furthermore, the variation could also be related to the less homogeneous loading degrees of Syloid AL-1 particles. In the case of the Syloid 244 particles the ITZ-loading degree exceeded the theoretical monolayer capacity (14.0 w-%), which can be attributed to the high pore volume (1.420 cm^3/g) and large pore size (19.0 nm) of the particles.

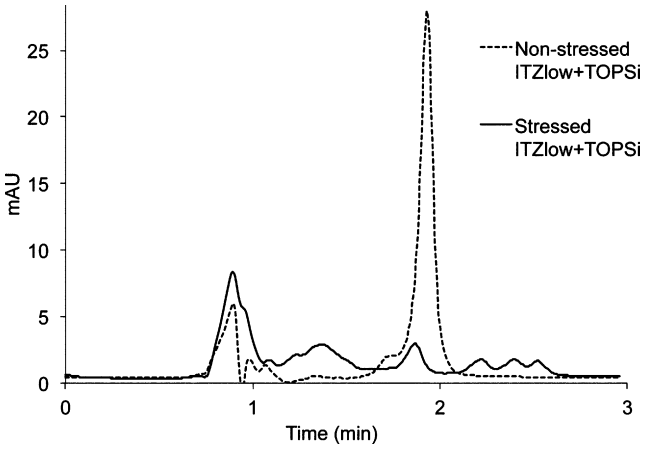

Fig. 4. HPLC chromatograms of stressed (3 months, 40 °C and 70% RH) ITZlow + TOPSi and non-stressed ITZlow + TOPSi. The loaded particles were dissolved in MeOH prior to HPLC measurements.

After storing the particles under stressed conditions (40 °C/70% RH) for 3 months, only a small decrease in the amount of ITZ was observed for the Syloid particles (21.3, 19.1, 30.4, and 16.6 w-% for ITZhigh + SylAL-1, ITZlow + SylAL-1, ITZhigh + Syl244, and ITZlow + Syl244, respectively) compared to the non-stressed samples (Table 2). Surprisingly, the amount of ITZ found in the PSi particles after storage was very low compared to the non-stressed samples. This is attributed to the chemical degradation of ITZ during the storage of the loaded PSi particles (Fig. 4).

Overall, we have shown that the structures of the mesoporous materials and the loading parameters are crucial factors for efficient drug loading. The surface chemistry, pore geometry and particle size of the mesoporous particles were the most crucial physical properties when loading ITZ into the non-ordered mesoporous silica and PSi particles. Although important, the surface area, the pore volume and the pore diameter affected to a lesser extent the loading efficiency of ITZ into those particles. However, more studies are still needed to verify the most optimal loading parameters to achieve maximum loading of a particular drug molecule with certain types of particles.

3.3. Release of ITZ from the mesoporous microparticles

The ITZ release from all the loaded mesoporous microparticles was faster than the dissolution of pure ITZ at pH 1.2 (Figs. 5 and 6), as a result of the amorphous form of ITZ when loaded to the mesoporous materials (Mellaerts et al., 2007, 2008a,b). The rapid release of the drug is a result of the fast dissolution of the confined molecules, followed by a fast diffusion into the bulk medium. This is also in very good agreement with both the DSC and XRPD results (Figs. 2 and 3, respectively). The ITZ release profiles of the non-ordered mesoporous materials used in this study are also in line with those obtained for the ordered mesoporous silica reported elsewhere (Mellaerts et al., 2007, 2008a,b). However, in contrast to those studies, we did not use any dissolution enhancing surfactants, such as sodium lauryl sulfate. Enhanced dissolution of loaded ITZ from the mesoporous materials can be achieved in the absence of surfactants and with non-ordered mesoporous materials.

Comparison of the loaded mesoporous materials show very fast initial drug release profiles; 50% of the loaded ITZ was dissolved within 3 min and more than 80% of the drug was dissolved after 5 min comparing to only 14% of pure ITZ. The ITZ release was the fastest when loaded into TCPSi and Syloid AL-1 microparticles. The drug release from Syloid 244 and TOPSi was slightly slower than

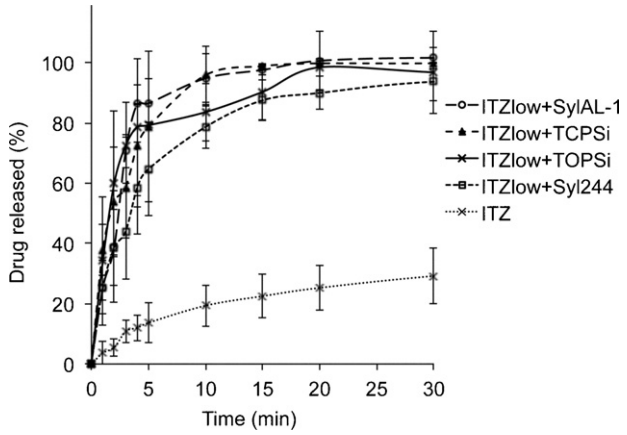

Fig. 5. Comparison of the release profiles of ITZ from silica and silicon microparticles, loaded at low drug concentration solutions, at pH 1.2 and 37 °C (lines $n \geq 4$, mean ± SD). The dissolution curve of bulk ITZ are also presented as reference.

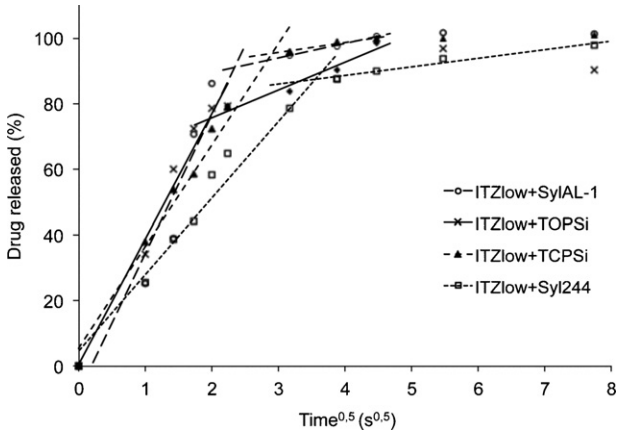

Fig. 7. Higuchi model analysis for the release of ITZ at pH 1.2 from ITZlow + TOPSi, ITZlow + TCPSi, ITZlow + SylAL-1, and ITZlow + Syl244 particles.

TCPSi and Syloid AL-1, but was still significantly faster compared to bulk ITZ.

Interestingly, when comparing the loading methods of ITZ into mesoporous silica particles performed at low and high ITZ concentrations, it could be observed that for the same type of particles the faster drug release profiles were obtained for loadings with the lower amounts of drug (Fig. 6). The surface chemistry of the mesoporous material may also decrease the drug release rate as a result of the interactions between the drug and the functional groups of the mesopores (Limnell et al., 2007). On the other hand, when the drug loading concentration is rather high, partial pore blockage can take place during the release experiments due to drug crystallization on top of the pores (Riikonen et al., 2009), particularly for particles with large pore sizes (Syloid 244), which may also retard the drug release.

All the particles released about 100% of ITZ during the dissolution test (120 min), whereas only 52% of pure ITZ was released (data not shown). The lowest required sampling time to reach 95% release from the particles was 10, 15, and 20 min for TCPSi, ITZlow + SylAL-1 and ITZ + TOPSi, respectively. For the samples ITZhigh + Syl244, ITZlow + Syl244 and ITZhigh + SylAL-1 the 95% release was achieved after 90 and 60 (data not shown), and 30 min, respectively. In previous studies the larger particle size has been related to slower drug release rate (Aerts et al., 2007; Böttcher et al., 1998; Qu et al., 2006a). However, in this study we did not observe a significant effect of the particle size on the drug release kinetics.

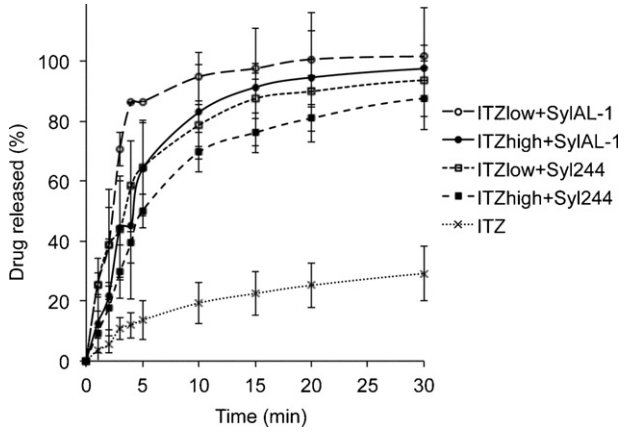

Fig. 6. Comparison of the release profiles of ITZ from silica microparticles, loaded at low and high drug concentration solutions, at pH 1.2 and 37 °C (lines $n \geq 4$, mean ± SD). The dissolution curve of bulk ITZ are also presented as reference.

In general the ITZ release from Syloid AL-1 particles was faster than from Syloid 244 particles. Besides the reasons discussed above, the differences observed in the drug release of Syloid AL-1 compared to Syloid 244 could also be explained by the smaller pore size of the former. Drug release from amorphous silicon dioxides with wide range of pore diameters (2–21 nm) has been shown to be slower for particles with larger pores due drug entrapment (Yang et al., 1979). Furthermore, adsorbed ITZ on the external surface of mesoporous silica has been shown to enhance the drug dissolution (Van Speybroeck et al., 2009), which could support the results obtained for the Syloid AL-1. In the case of PSi particles, the different release profiles are most likely linked to the different surface chemistries of the particles and their interactions with drug molecules during dissolution (Muñoz et al., 2003; Salonen et al., 2005; Song et al., 2005).

Interestingly, although the physical properties (pore volume, surface area and pore diameter) of TCPSi particles were more close to Syloid 244 than Syloid AL-1 (Table 1), similar ITZ release profiles were obtained for TCPSi and ITZlow + SylAL-1 particles. This could be explained by the lower loading degrees of ITZ in the TCPSi particles compared to the ITZlow + SylAL-1 particles, and also by the different particle surface chemistries.

To better compare the drug release profiles obtained at pH 1.2, the results of Fig. 5 were fitted with the Higuchi model (Higuchi, 1963), which can be used to describe the release of a drug from an insoluble matrix, and has previously been employed for the evaluation of the drug release kinetics from mesoporous silica particles (Andersson et al., 2004; Kim et al., 2006; Qu et al., 2006b). The mathematical model is based on Fickian diffusion and it describes the amount of released drug, f_t, at a certain time, t [Eq. (1)]:

$$f_t = K_H\sqrt{t} \quad (1)$$

where K_H is the Higuchi dissolution constant. This model was selected over, for example, Korsmeyer–Peppas and the first-order kinetics models, because it gave the best fittings for the dissolution data in this study. The dissolution data of the mesoporous materials fitted with the Higuchi model are shown in Fig. 7 and Table 3. Accordingly, the drug was released from the particles by diffusion in a two-step drug release profile, which is in very good agreement with previous reports (Andersson et al., 2004; Kim et al., 2006; Qu et al., 2006b). The two-step drug release indicates that the slower release rate in the second stage is related to chemical bonding between the drug and the surface of the mesoporous materials, whereas in the first stage the physically entrapped drug molecule is released faster (Kim et al., 2006). In addition, the drug molecules located on or near the surface of the porous material can be released fast due to the instant dissolution and release in

Table 3
Higuchi release constants (K_H) and correlation coefficients (R^2) for the ITZ release from ITZlow + TOPSi, ITZlow + TCPSi, ITZlow + SylAL-1, and ITZlow + Syl244 particles.

Particles	First step			Second step		
	Duration	k_H	R^2	Duration	K_H	R^2
ITZlow + SylAL-1	0–5 min	42.2	0.9313	5–20 min	6.2	0.9643
ITZlow + TOPSi	0–5 min	38.2	0.9731	5–20 min	8.5	0.9476
ITZlow + TCPSi	0–10 min	30.9	0.9746	10–20 min	3.0	0.9398
ITZlow + Syl244	0–15 min	23.3	0.9658	15–60 min	2.6	0.9629

the medium, whereas the drug molecules packed deeper inside the pore network are released much slower (Doadrio et al., 2004; Van Speybroeck et al., 2009). The Higuchi release constants suggest that the drug release from TOPSi and Syloid AL-1 was faster than from TCPSi, but the slow release step started earlier with TOPSi and Syloid AL-1 (at 5 min) than with TCPSi (at 10 min), which slowed down the overall release from TOPSi and Syloid AL-1 (Table 3). Because the rapid release during the first step with TCPSi lasted for 10 min, TCPSi particles released 95% of ITZ within 10 min, while 95% release took longer for all the other particles. The first step lasted the longest with Syloid 244, but due to the lowest release constants, the overall release profile was the slowest with these particles.

The dissolution profiles of ITZ release from the mesoporous particles after being kept under stressed conditions for 3 months (40 °C/70% RH) showed only a slight decrease in the drug release rate for the Syloids compared to the non-stressed samples (Fig. 8), evidencing physical stability of the formulations similar to those reported for the ordered mesoporous silica (Van Speybroeck et al., 2009). However, in the present study the storage conditions used were harsher than those reported before. In contrast to the silica particles, a significant decrease in the release profiles of ITZ was observed from the stressed PSi particles when compared with the non-stressed samples. This can be explained due to the almost complete chemical degradation of ITZ in the TCPSi and TOPSi (Fig. 4) particles after storage, whereas only slight degradation of ITZ from the Syloid particles was observed in the HPLC chromatograms (data not shown). Although the phenomenon is not fully understood yet, it is probable that the surface chemistry of PSi induced some reactions during storage, which could have led to the chemical degradation of the ITZ molecules loaded inside the pores, or the increased moisture inside the pores could have also led to the release of great part of the loaded ITZ. We have previously reported that azo-based compounds (Laaksonen et al., 2007) undergo redox reactions when in contact to PSi surfaces. The ITZ molecule contains triazole-derivate groups which overtime and under high relative humidity and temperature could trigger reactions between the ITZ and the particle's pore walls leading to possible degradation of the drug molecule. ITZ has also several functional groups that are susceptible to oxidation. For example, the piperazine ring can degrade by oxidation; the dioxolane ring can go through oxidative scission; the ether group can oxidize into aldehydes, ketones, alcohols and carboxylic acids; and the methyl groups can hydroxylate into aldehydes and carboxylic acids and the benzyl ring can hydroxylate into phenol (Beule, 1996; Feng et al., 2001; Lhomme et al., 2007). After ITZ-loading the hydrophilicity of the PSi particles are slightly higher than of the silica particles due to the lower loading degree of ITZ in the PSi particles. Therefore, under stress conditions the PSi surface could also have more affinity for water than the silica particles which would contribute for an extended degree of oxidation of the ITZ molecule and its consequent degradation. Further studies are being undertaken to understand what chemical modifications are taking place during storage when ITZ is loaded into PSi microparticles. Despite of that, DSC results did not show any crystallization of ITZ during storage for any of the mesoporous materials (data not shown), and therefore drug recrystallization of the entrapped molecules seems to be ruled out in this case. Furthermore, FTIR studies did not evidence any surface structural changes in the particles after storage (data not shown). Nevertheless, in the case of PSi particles the water taken up during storage seemed to have extensively affected the drug-loaded carrier, leading to the chemical degradation of ITZ, which strongly contrasts earlier TCPSi storage studies when loaded with ibuprofen molecules (Limnell et al., 2007). These dissimilar results are likely to be caused by the different chemical structures of the drugs with different functional groups.

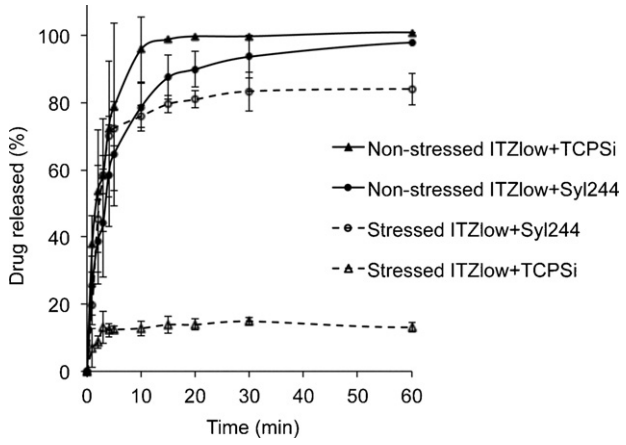

Fig. 8. Comparison of the release profiles of ITZ from ITZlow + TCPSi and ITZlow + Syl244 particles at pH 1.2 and 37 °C before and after storage under stress conditions (40 °C and 70% RH) (lines $n \geq 4$, mean ± SD).

4. Conclusions

The aim of this study was to evaluate the structural effects of mesoporous silicon and non-ordered mesoporous silica materials on the loading degrees and dissolution behavior of the poorly soluble drug itraconazole (ITZ). The release of ITZ at pH 1.2 from thermally carbonized porous silicon (TCPSi) and Syloid AL-1 microparticles was faster than from the thermally oxidized-PSi (TOPSi) and Syloid 244 particles. This was described as a result of smaller pore size of Syloid AL-1 compared to Syloid 244, and of the more favorable surface chemistry of TCPSi compared to TOPSi. Interestingly, the particle size did not affect the drug release kinetics. The adsorbed drug fraction was found to be non-crystalline in all the samples, even after 3 months storage at 40 °C and 70% RH, and resulted in a significant improvement in dissolution rate as compared to the crystalline ITZ. The surface structure of the mesoporous silica particles containing large amounts of silanol groups, together with the silica gel pore structure and the small particle size were revealed to be advantageous properties for the efficient loading of ITZ. On the other hand, the high pore volume was advantageous for high loading degree. Loadings at lower drug concentrations were demonstrated to be more suitable for a faster drug release than loadings at high drug concentrations. No major changes in the release profiles of ITZ were observed from Syloid samples after 3 months storage under the stressed conditions. In contrast, PSi

materials revealed to be inefficient to protect ITZ from chemical degradation during the storage. Encapsulation of ITZ into the non-ordered mesoporous silica and PSi is as efficient and promising as in the cases of ordered mesoporous silica materials (e.g., MCM-41 or SBA-15 materials), but caution is warranted in PSi use for longer storage times of ITZ. Non-ordered siliceous mesoporous materials, such as Syloids, are currently widely used as food additives and pharmaceutical excipients. Therefore, the non-ordered siliceous materials are also rather promising for physical stability and dissolution enhancement of drug formulations, which renders them alternatives for carriers of hydrophobic drug molecules. The physicochemical properties of the particles are the crucial parameters for the drug loading efficiency, the drug release kinetics, and the stability of loaded drug. By adjusting the drug loading parameters, the effects on both the drug loading efficiency and the drug release kinetics can be tailored.

Acknowledgements

Financial support from the Academy of Finland (grant no. 127099) and the University of Helsinki Research Funds is acknowledged. P.K. thanks the National Graduate School in Nanoscience for a PhD grant.

Appendix A. Supplementary data

Supplementary data associated with this article can be found, in the online version, at doi:10.1016/j.ijpharm.2011.05.021.

References

Aerts, C.A., Verraedt, E., Mellaerts, R., Depla, A., Augustijns, P., Van Humbeeck, J., Van den Mooter, G., Martens, J.A., 2007. Tunability of pore diameter and particle size of amorphous microporous silica for diffusive controlled release of drug compounds. J. Phys. Chem. C 111, 13404–13409.

Ahola, M., Kortesuo, P., Kangasniemi, I., Kiesvaara, J., Yli-Urpo, A., 2000. Silica xerogel carrier material for controlled release of toremifene citrate. Int. J. Pharm. 195, 219–227.

Ambrogi, V., Perioli, L., Marmottini, F., Giovagnoli, S., Esposito, M., Rossi, C., 2007. Improvement of dissolution rate of piroxicam by inclusion into MCM-41 mesoporous silicate. Eur. J. Pharm. Sci. 32, 216–222.

Ambrogi, V., Perioli, L., Marmottini, F., Accorsi, O., Pagano, C., Ricci, M., Rossi, C., 2008. Role of mesoporous silicates on carbamazepine dissolution rate enhancement. Micropor. Mesopor. Mater. 113, 445–452.

Andersson, J., Rosenholm, J., Areva, S., Linden, M., 2004. Influences of material characteristics on ibuprofen drug loading and release profiles from ordered micro-and mesoporous silica matrices. Chem. Mater. 16, 4160–4167.

Beck, J., Vartuli, J., Roth, W., Leonowicz, M., Kresge, C., Schmitt, K., Chu, C., Olson, D., Sheppard, E., 1992. A new family of mesoporous molecular sieves prepared with liquid crystal templates. J. Am. Chem. Soc. 114, 10834–10843.

Beule, K.D., 1996. Itraconazole: pharmacology, clinical experience and future development. Int. J. Antimicrob. Agents 6, 175–181.

Bimbo, L.M., Mäkilä, E., Laaksonen, T., Lehto, V.P., Salonen, J., Hirvonen, J., Santos, H.A., 2011. Drug permeation across intestinal epithelial cells using porous silicon nanoparticles. Biomaterials 32, 2625–2633.

Bimbo, L.M., Sarparanta, M., Santos, H.A., Airaksinen, A.J., Mäkilä, E., Laaksonen, T., Peltonen, L., Lehto, V.P., Hirvonen, J., Salonen, J., 2010. Biocompatibility of thermally hydrocarbonized porous silicon nanoparticles and their biodistribution in rats. ACS Nano 4, 3023–3032.

Böttcher, H., Slowik, P., Süß, W., 1998. Sol–gel carrier systems for controlled drug delivery. J. Sol–Gel Sci. Technol. 13, 277–281.

Charnay, C., Begu, S., Tourne-Peteilh, C., Nicole, L., Lerner, D., Devoisselle, J., 2004. Inclusion of ibuprofen in mesoporous templated silica: drug loading and release property. Eur. J. Pharm. Biopharm. 57, 533–540.

Chen, J.F., Ding, H.M., Wang, J.X., Shao, L., 2004. Preparation and characterization of porous hollow silica nanoparticles for drug delivery application. Biomaterials 25, 723–727.

Doadrio, A., Sousa, E., Doadrio, J., Pérez Pariente, J., Izquierdo-Barba, I., 2004. Mesoporous SBA-15 HPLC evaluation for controlled gentamicin drug delivery. J. Control. Release 97, 125–132.

Feng, W., Liu, H., Chen, G., Malchow, R., Bennett, F., Lin, E., Pramanik, B., Chan, T.M., 2001. Structural characterization of the oxidative degradation products of an antifungal agent SCH 56592 by LC–NMR and LC–MS. J. Pharm. Biomed. Anal. 25, 545–557.

Fisher, K.A., Huddersman, K.D., Taylor, M.J., 2003. Comparison of micro- and mesoporous inorganic materials in the uptake and release of the drug model fluorescein and its analogues. Chemistry 9, 5873–5878.

Foraker, A.B., Walczak, R.J., Cohen, M.H., Boiarski, T.A., Grove, C.F., Swaan, P.W., 2003. Microfabricated porous silicon particles enhance paracellular delivery of insulin across intestinal Caco-2 cell monolayers. Pharm. Res. 20, 110–116.

Hancock, B.C., Carlson, G.T., Ladipo, D.D., Langdon, B.A., Mullarney, M.P., 2002. Comparison of the mechanical properties of the crystalline and amorphous forms of a drug substance. Int. J. Pharm. 241, 73–85.

Heikkilä, T., Salonen, J., Tuura, J., Hamdy, M., Mul, G., Kumar, N., Salmi, T., Murzin, D.Y., Laitinen, L., Kaukonen, A., 2007a. Mesoporous silica material TUD-1 as a drug delivery system. Int. J. Pharm. 331, 133–138.

Heikkilä, T., Salonen, J., Tuura, J., Kumar, N., Salmi, T., Murzin, D.Y., Hamdy, M.S., Mul, G., Laitinen, L., Kaukonen, A.M., Hirvonen, J., Lehto, V.P., 2007b. Evaluation of mesoporous TCPSi, MCM-41, SBA-15, and TUD-1 materials as API carriers for oral drug delivery. Drug Deliv. 14, 337–347.

Higuchi, T., 1963. Mechanism of sustained-action medication: Theoretical analysis of rate of release of solid drugs dispersed in solid matrices. J. Pharm. Sci. 52, 1145–1149.

Horcajada, P., Rámila, A., Pérez-Pariente, J., Vallet-Regí, M., 2004. Influence of pore size of MCM-41 matrices on drug delivery rate. Micropor. Mesopor. Mater. 68, 105–109.

Horcajada, P., Rámila, A., Férey, G., Vallet-Regí, M., 2006. Influence of superficial organic modification of MCM-41 matrices on drug delivery rate. Solid State Sci. 8, 1243–1249.

Jesionowski, T., Pokora, M., Sobaszkiewicz, K., Pernak, J., 2004. Preparation and characterization of functionalized precipitated silica SYLOID® 244 using ionic liquids as modifiers. Surf. Interface Anal. 36, 1491–1496.

Kaukonen, A.M., Laitinen, L., Salonen, J., Tuura, J., Heikkila, T., Limnell, T., Hirvonen, J., Lehto, V.P., 2007. Enhanced in vitro permeation of furosemide loaded into thermally carbonized mesoporous silicon (TCPSi) microparticles. Eur. J. Pharm. Biopharm. 66, 348–356.

Kilpeläinen, M., Riikonen, J., Vlasova, M.A., Huotari, A., Lehto, V.P., Salonen, J., Herzig, K.H., Järvinen, K., 2009. In vivo delivery of a peptide, ghrelin antagonist, with mesoporous silicon microparticles. J. Control. Release 137, 166–170.

Kim, H.J., Ahn, J.E., Haam, S., Shul, Y.G., Song, S.Y., Tatsumi, T., 2006. Synthesis and characterization of mesoporous Fe/SiO_2 for magnetic drug targeting. J. Mater. Chem. 16, 1617–1621.

Kortesuo, P., Ahola, M., Kangas, M., Kangasniemi, I., Yli-Urpo, A., Kiesvaara, J., 2000. In vitro evaluation of sol-gel processed spray dried silica gel microspheres as carrier in controlled drug delivery. Int. J. Pharm. 200, 223–229.

Kortesuo, P., Ahola, M., Kangas, M., Leino, T., Laakso, S., Vuorilehto, L., Yli-Urpo, A., Kiesvaara, J., Marvola, M., 2001. Alkyl-substituted silica gel as a carrier in the controlled release of dexmedetomidine. J. Control. Release 76, 227–238.

Laaksonen, T., Santos, H., Vihola, H., Salonen, J., Riikonen, J., Heikkilä, T., Peltonen, L., Kumar, N., Murzin, D.Y., Lehto, V.-P., Hirvonen, J., 2007. Failure of MTT as a toxicity testing agent for mesoporous silicon microparticles. Chem. Res. Toxicol. 20, 1913–1918.

Limnell, T., Santos, H., Mäkilä, E., Heikkilä, T., Salonen, J., Murzin, D.Y., Kumar, N., Laaksonen, T., Peltonen, L., Hirvonen, J., 2011. Drug delivery formulations of ordered and non-ordered mesoporous silica: comparison of three drug loading methods. J. Pharm. Sci., doi:10.1002/jps.22577.

Limnell, T., Riikonen, J., Salonen, J., Kaukonen, A.M., Laitinen, L., Hirvonen, J., Lehto, V.P., 2007. Surface chemistry and pore size affect carrier properties of mesoporous silicon microparticles. Int. J. Pharm. 343, 141–147.

Lhomme, L., Brosillon, S., Wolbert, D., 2007. Photocatalytic degradation of triazole pesticide, cyproconazole, in water. J. Photochem. Photobiol. A 188, 34–42.

Mellaerts, R., Mols, R., Jammaer, J.A.G., Aerts, C.A., Annaert, P., Van Humbeeck, J., Van den Mooter, G., Augustijns, P., Martens, J.A., 2008b. Increasing the oral bioavailability of the poorly water soluble drug itraconazole with ordered mesoporous silica. Eur. J. Pharm. Biopharm. 69, 223–230.

Mellaerts, R., Aerts, C.A., Van Humbeeck, J., Augustijns, P., Van den Mooter, G., Martens, J.A., 2007. Enhanced release of itraconazole from ordered mesoporous SBA-15 silica materials. Chem. Commun. (Cambridge, U.K.), 1375–1377.

Mellaerts, R., Jammaer, J.A., Van Speybroeck, M., Chen, H., Van Humbeeck, J., Augustijns, P., Van den Mooter, G., Martens, J.A., 2008a. Physical state of poorly water soluble therapeutic molecules loaded into SBA-15 ordered mesoporous silica carriers: a case study with itraconazole and ibuprofen. Langmuir 24, 8651–8659.

Monkhouse, D.C., Lach, J.L., 1972. Use of adsorbents in enhancement of drug dissolution, I and II. J. Pharm. Sci. 61, 1430–1441.

Muñoz, B., Rámila, A., Pérez-Pariente, J., Díaz, I., Vallet-Regí, M., 2003. MCM-41 organic modification as drug delivery rate regulator. Chem. Mater. 15, 500–503.

Nakanishi, K., Takahashi, R., Nagakane, T., Kitayama, K., Koheiya, N., Shikata, H., Soga, N., 2000. Formation of hierarchical pore structure in silica gel. J. Sol–Gel Sci. Technol. 17, 191–210.

Narurkar, A.N., Jarowski, C.I., 1983. Dissolution rates of prednisolone triturations using porous and non-porous silicas. I. Pilot oral absorption study in dogs. Drug Dev. Ind. Pharm. 9, 999–1010.

Peeters, J., Neeskens, P., Tollenaere, J.P., Van Remoortere, P., Brewster, M.E., 2002. Characterization of the interaction of 2-hydroxypropyl-beta-cyclodextrin with itraconazole at pH 2, 4, and 7. J. Pharm. Sci. 91, 1414–1422.

Qu, F., Zhu, G., Lin, H., Zhang, W., Sun, J., Li, S., Qiu, S., 2006a. A controlled release of ibuprofen by systematically tailoring the morphology of mesoporous silica materials. J. Solid State Chem. 179, 2027–2035.

Qu, F., Zhu, G., Huang, S., Li, S., Qiu, S., 2006b. Effective controlled release of captopril by silylation of mesoporous MCM-41. ChemPhysChem 7, 400–406.

Radin, S., Ducheyne, P., Kamplain, T., Tan, B.H., 2001. Silica sol–gel for the controlled release of antibiotics. I. Synthesis, characterization, and in vitro release. J. Biomed. Mater. Res. A 57, 313–320.
Rigby, S., Fairhead, M., Van Der Walle, C., 2008. Engineering silica particles as oral drug delivery vehicles. Curr. Pharm. Des. 14, 1821–1831.
Riikonen, J., Mäkilä, E., Salonen, J., Lehto, V.P., 2009. Determination of the physical state of drug molecules in mesoporous silicon with different surface chemistries. Langmuir 25, 6137–6142.
Rosenholm, J.M., Lindén, M., 2008. Towards establishing structure–activity relationships for mesoporous silica in drug delivery applications. J. Control. Release 128, 157–164.
Rowe, R.C., Sheskey, P.J., Weller, P.J., 2003. Handbook of pharmaceutical excipients. Pharmaceutical Press, London.
Salonen, J., Laine, E., Niinistö, L., 2002. Thermal carbonization of porous silicon surface by acetylene. J. Appl. Phys. 91, 456.
Salonen, J., Lehto, V.P., Laine, E., 1997a. Thermal oxidation of free-standing porous silicon films. Appl. Phys. Lett. 70, 637.
Salonen, J., Lehto, V.P., Laine, E., 1997b. The room temperature oxidation of porous silicon. Appl. Surf. Sci. 120, 191–198.
Salonen, J., Kaukonen, A.M., Hirvonen, J., Lehto, V.P., 2008. Mesoporous silicon in drug delivery applications. J. Pharm. Sci. 97, 632–653.
Salonen, J., Laitinen, L., Kaukonen, A.M., Tuura, J., Bjorkqvist, M., Heikkila, T., Vaha-Heikkila, K., Hirvonen, J., Lehto, V.P., 2005. Mesoporous silicon microparticles for oral drug delivery: loading and release of five model drugs. J. Control. Release 108, 362–374.
Salonen, J., Lehto, V., 2008. Fabrication and chemical surface modification of mesoporous silicon for biomedical applications. Chem. Eng. J. 137, 162–172.
Santos, E.M., Radin, S., Ducheyne, P., 1999. Sol–gel derived carrier for the controlled release of proteins. Biomaterials 20, 1695–1700.
Santos, H.A., Riikonen, J., Salonen, J., Mäkilä, E., Heikkilä, T., Laaksonen, T., Peltonen, L., Lehto, V., Hirvonen, J., 2010. In vitro cytotoxicity of porous silicon microparticles: Effect of the particle concentration, surface chemistry and size. Acta Biomater. 6, 2721–2731.
Song, S.W., Hidajat, K., Kawi, S., 2005. Functionalized SBA-15 materials as carriers for controlled drug delivery: influence of surface properties on matrix–drug interactions. Langmuir 21, 9568–9575.
Van Speybroeck, M., Barillaro, V., Thi, T.D., Mellaerts, R., Martens, J., Van Humbeeck, J., Vermant, J., Annaert, P., Van den Mooter, G., Augustijns, P., 2009. Ordered mesoporous silica material SBA-15: a broad-spectrum formulation platform for poorly soluble drugs. J. Pharm. Sci. 98, 2648–2658.
Van Speybroeck, M., Mols, R., Mellaerts, R., Thi, T.D., Martens, J.A., Humbeeck, J.V., Annaert, P., Mooter, G.V., Augustijns, d.P., 2010. Combined use of ordered mesoporous silica and precipitation inhibitors for improved oral absorption of the poorly soluble weak base itraconazole. Eur. J. Pharm. Biopharm. 75, 354–365.
Wang, S., 2009. Ordered mesoporous materials for drug delivery. Micropor. Mesopor. Mater. 117, 1–9.
Wang, F., Hui, H., Barnes, T.J., Barnett, C., Prestidge, C.A., 2010. Oxidized mesoporous silicon microparticles for improved oral delivery of poorly soluble drugs. Mol. Pharm. 7, 227–236.
Wang, S., Li, H.T., 2006. Structure directed reversible adsorption of organic dye on mesoporous silica in aqueous solution. Micropor. Mesopor. Mater. 97, 21–26.
W.R., Grace, Co.-Conn., 2006. Products and Applications. http://www.grace.com/EngineeredMaterials/ProductsAndApplications/Default.aspx (accessed 14.03.2011).
Yang, K.Y., Glemza, R., Jarowski, C.I., 1979. Effects of amorphous silicon dioxides on drug dissolution. J. Pharm. Sci. 68, 560–565.
Zhao, D., Feng, J., Huo, Q., Melosh, N., Fredrickson, G.H., Chmelka, B.F., Stucky, G.D., 1998. Triblock copolymer syntheses of mesoporous silica with periodic 50–300 Å pores. Science 279, 548.
Zhao, X., Lu, G., Whittaker, A., Millar, G., Zhu, H., 1997. Comprehensive study of surface chemistry of MCM-41 using 29Si CP/MAS NMR, FTIR, pyridine–TPD, and TGA. J. Phys. Chem. B 101, 6525–6531.
Zhuravlev, L., 1987. Concentration of hydroxyl groups on the surface of amorphous silicas. Langmuir 3, 316–318.
Zhuravlev, L.T., 2000. The surface chemistry of amorphous silica. Zhuravlev model. Colloids Surf. A: Physicochem. Eng. Aspects 173, 1–38.